Influence of GM on Surf-Riding and Broaching of the Fishing Vessel

Liwei Yu[1(✉)], Ning Ma[2], Shuqing Wang[1], and Tinghao Wang[2]

[1] Shandong Provincial Key Laboratory of Ocean Engineering,
Ocean University of China, Qingdao, China
`yuliwei@ouc.edu.cn`
[2] State Key Laboratory of Ocean Engineering,
Shanghai Jiao Tong University, Shanghai, China

Abstract. The influence of GM on surf-riding and broaching of the ITTC A2 fishing vessel (Length between perpendiculars: 34.5 m, Breadth: 7.60 m, Draught: 2.65 m) are investigated using a 6-DOF numerical model. The numerical model is validated by comparisons with the model experiment provided in the literature. Then, through numerical simulations in following and quartering seas with different GM values, it is found that the threshold Froude number Fn_{th} of surf-riding and broaching is around $Fn_{th} = 0.39$ for all GM values, and the ship tends to capsize as the wave direction growing. The change on GM value has significant influence on the occurrence of broaching and capsizing. The ship is vulnerable to capsizing when GM = 0.8 m. However, Almost no capsizing occurs even in large quartering waves when GM = 1.2 m.

Keywords: Broaching · Surf-riding · GM · Fishing vessel design

1 Introduction

In heavy following and quartering seas, ships can be accelerated to the wave celerity under the interaction among thrust, resistance and wave surging force. Under this circumstance, the ship's heading may change abruptly with possible loss of stability. These phenomena are referred as surf-riding and broaching. They are the major causes for the stability failure of fishing vessels in following and quartering seas.

Researches on surf-riding and broaching are attempted firstly by Davidson [1] and Grim [3] around 1950s. Since then, developments on computer technologies have promoted the numerical simulations on surf-riding and broaching with different levels of model complexity [12, 13, 16, 17]. Nonlinear dynamics approaches [7, 10, 11] and model experiments [4, 14, 15] also contributed significantly to the understanding of their mechanisms as well as the establishment of proper criteria. Under the support of these works, IMO subcommittee on ship design and construction (SDC) proposed the draft guidelines on the second generation intact stability criteria as the amendment to Part B of the 2008 IS code [6]. In this draft criteria, a three-level approach is introduced for the assessment of five stability failure modes including surf-riding and broaching. According to the sample ship calculation [2], most of the fishing vessels cannot pass either level 1 or level 2 criteria of surf-riding and broaching. Thus, for most of the

fishing vessels, design improvement or ship-specific operation guidance is required for the avoidance of surf-riding and broaching in following and quartering seas. For the avoidance of surf-riding through design improvements, bilge keel and changing of the longitudinal position of ship's center of buoyancy (COB) were proved to be effective [18, 19].

In the design and operation stage, the center of gravity (COG), more precisely the metacentric height GM, is the fundamental factor for the stability of ships in waves. However, there is few investigation on the influence of GM on surf-riding and broaching. Therefore, the influence of GM on surf-riding and broaching should be investigated, which may benefit the establishment of the ship-specific operation guidance for fishing vessels failed in Level 1 and 2 criteria.

Therefore in this paper, the effect of the GM on surf-riding and broaching are investigated using a 6-DOF numerical model proposed by Yu et al. [16]. The ITTC A2 fishing vessel are chosen as the subject ship [8]. Numerical simulations of surf-riding and broaching in following and quartering seas with various speeds, wave directions and GM values are conducted. Based on results of the numerical simulation, the influence of the GM on surf-riding and broaching is investigated.

2 Numerical Model

The numerical model for the simulation of surf-riding and broaching is a 6-DOF maneuvering model considering the nonlinearity of restoring and F-K forces as well as rudder and propeller dynamics.

2.1 Coordinate System

Three coordinate systems, the earth fixed coordinate O_e-$x_e y_e z_e$, the body fixed coordinate O-xyz and the horizontal body axes coordinate O_h-$x_h y_h z_h$ are used as shown in Fig. 1. The origin O is chosen as the ship center of gravity. The position, velocity and force vectors are defined as:

$$\boldsymbol{\eta} = [x, y, z, \phi, \theta, \psi]^T; \boldsymbol{v} = [u, v, w, p, q, r]^T; \boldsymbol{f} = [X, Y, Z, K, M, N]^T \tag{1}$$
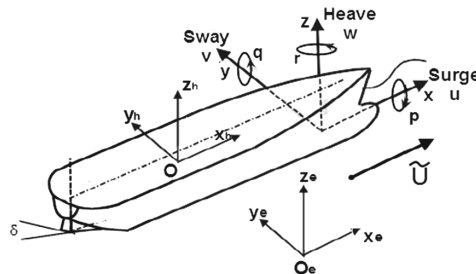

Fig. 1. Definition of coordinate system and ship motions

The ship forward speed is $\tilde{U} = \sqrt{u^2 + v^2}$. The velocity vector $\mathbf{v}$ which is defined in body-fixed coordinate is transferred to earth-fixed coordinate:

$$\dot{\eta} = \left[\dot{x}, \dot{y}, \dot{z}, \dot{\phi}, \dot{\theta}, \dot{\psi}\right]^T = [U, V, W, P, Q, R]^T = \begin{bmatrix} \mathbf{R}_{3\times3} & \mathbf{0}_{3\times3} \\ \mathbf{0}_{3\times3} & \mathbf{Q}_{3\times3} \end{bmatrix} \mathbf{v} \qquad (2)$$

Where U, V, W, P, Q and R is the velocity in the earth-fixed coordinate, $\mathbf{R}_{3\times3}$ and $\mathbf{Q}_{3\times3}$ are transfer matrixes as described in Yu et al. [16].

2.2 6-DOF Maneuvering Model

The 6-DOF maneuvering model considering roll, heave and pitch motions is formulated as Eq. (3).

$$
\begin{aligned}
(m+m_x)\dot{u} - (m+m_y)vr &= X_H + X_\delta + X_w - X_R + X_P \\
-(m+m_x)uv - (m+m_y)\dot{v} &= Y_H + Y_\delta \\
m\dot{w} &= F_3^{res}(t) + F_3^{FK}(t) + F_3^{rad}(t) \\
(I_x + J_x)\dot{p} + B_v p &= F_4^{res}(t) + F_4^{FK}(t) + F_4^{rad}(t) + F_4^{dif}(t) + (K_\delta - z_H Y_H) \\
I_y\dot{q} &= F_5^{res}(t) + F_5^{FK}(t) + F_5^{rad}(t) \\
-(I_z + J_z)\dot{r} &= N_H + N_\delta
\end{aligned}
\qquad (3)
$$

Where m, $m_{x,y,z}$, $I_{x,y,z}$, and $J_{x,y,z}$ represent the ship mass, added mass, moment of inertia and added moment of inertia. $(X_\delta, Y_\delta, N_\delta)$, X_w, X_R and X_P are defined as rudder force, wave surge force, resistance and propeller thrust respectively. B_v is the roll viscous damping estimated by the Ikeda's semi-empirical method [5]. z_H is the vertical position of acting point of Y_H. (X_H, Y_H, N_H) is the hull hydrodynamic force, while $F_i^{res}(t)$, $F_i^{FK}(t)$, $F_i^{rad}(t)$ and $F_i^{dif}(t)$ stand for the nonlinear restoring forces, F-K, radiation and diffraction forces.

$$
\begin{aligned}
X_w &= F_1^{res}(t) + F_1^{FK}(t) \\
X_R &= r_1\tilde{U} + r_2\tilde{U}^2 + r_3\tilde{U}^3 \\
X_H &= X_{vv}v^2 + X_{vr}vr + X_{rr}r^2 \\
Y_H &= -\bar{Y}_V v - \bar{Y}_R R - Y_{vvr}v^2 r - Y_{vrr}vr^2 - Y_{vvv}v^3 - Y_{rrr}r^3 \\
N_H &= -\bar{N}_V v - \bar{N}_R R - N_{vvr}v^2 r - N_{vrr}vr^2 - N_{vvv}v^3 - N_{rrr}r^3 \\
F_i^{rad}(t) &= -\sum_{j=3}^{5} \mu_{ij}(\infty)\dot{v}_j(t), \quad i = 3, 5 \\
F_4^{rad}(t) &= -\sum_{j=3}^{5} \int_0^t R_{4j}(t-\tau)v_j(\tau)d\tau, \quad F_4^{dif}(t) = \int_{-\infty}^t Q_4(t-\tau)\alpha(\tau)d\tau
\end{aligned}
\qquad (4)
$$

Where r_1, r_2, r_3 are the fitting coefficients of the resistance curve. Y_v, N_r etc.are linear derivatives of sway force and yaw moment. X_{vv}, Y_{vvr}, N_{vvr} etc. are nonlinear derivatives of surge, sway force and yaw moment. According to the IRF approach, the radiation and diffraction forces $F_i^{rad}(t)$, $F_i^{dif}(t)$ are calculated in frequency domain by the

STF method [9] and transferred into time domain using the retardation function R_{ij} and Q_i. Since the encounter frequency is small when surf-riding occurs, the diffraction and radiation forces for heave and pitch motions are ignored in this calculation. The propeller and rudder forces are calculated as in Yu et al. [17].

2.3   Nonlinear Restoring and F-K Forces

The nonlinear restoring and F-K forces are calculated through pressure integration on the instantaneous wetted surfaces [19]. During the calculation, the hull and upper deck consist of several Non-Uniform Rational B-Splines (NURBS) surfaces as demonstrated in Fig. 2. Each surface has an area of A_i, a central point $r_i = (x_i, y_i, z_i)$ with a normal vector $n_i = (n_{1i}, n_{2i}, n_{3i})$ in body-fixed axis. The restoring and Froude-Krylov forces are calculated as:

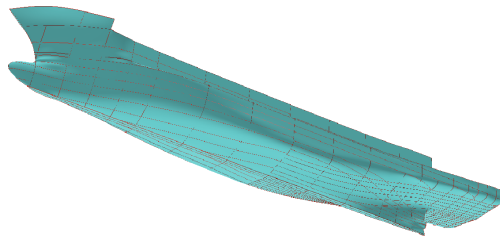**Fig. 2.** Hull NURBS surface of ITTC ship A2

$$F_j^{res} = \sum_{i=1}^{N^*} A_i P_{res}(\boldsymbol{r}_i) n_{ji}^h - mg \cos \theta \cos \phi \quad (j = 3)$$

$$F_j^{res} = \sum_{i=1}^{N^*} A_i P_{res}(\boldsymbol{r}_i) n_{ji}^h \times (r_G - \boldsymbol{r}_i^h) \quad (j = 4, 5)$$

$$(1)$$

Where the restoring pressure $P_{res}(r_i^h)$ are given by:

$$P_{res}(\boldsymbol{r}_i) = \rho g(d(x_i^e, t) - z_i^e) \tag{2}$$

Where the instantaneous draft $d(x_i, t)$ is calculated as:

$$d(x_i^e, t) = d_0 + \alpha(t) = d_0 + A_w \cos(\omega_e t - k(x_i^e \cos \chi + y_i^e \sin \chi)) \tag{3}$$

Superscript (h) and (e) indicates vectors in the horizontal body axes coordinate $O\text{-}X_h Y_h Z_h$ and the earth-fixed coordinate $O_e\text{-}X_e Y_e Z_e$.

3 Numerical Simulations

3.1 Subject Ship and Calculation Cases

The subject ship used for the numerical simulation is the ITTC ship A2 fishing vessel [8]. Main particulars of the ship, rudder and their models are shown in Table 1. The autopilot system is modelled as follows:

Table 1. Main particulars of ITTC ship A2

Ship		1/15 model
Length between perpendiculars, L_{pp}(m)	34.5	2.3
Breadth, B(m)	7.60	0.507
Depth, D(m)	3.07	0.205
Fore draught, d_f(m)	2.5	0.166
Aft draught, d_a(m)	2.8	0.176
Mean draught, d(m)	2.65	0.186
Block coefficient, C_B	0.597	0.597
Radius of gyration, roll, k_{xx}/L_{pp}	0.108	0.108
Radius of gyration, pitch yaw, k_{yy}/L_{pp}, k_{zz}/L_{pp}	0.302	0.302
Longitudinal position of the center of Buoyancy, L_{CB}(m)	1.31 m aft	0.087 m aft
Longitudinal position of the center of Floatation, L_{CF}(m)	3.94 m aft	0.263 m aft
Metacentric height, GM(m)	1.00	0.0667
Natural roll period, T_R(s)	7.4	1.9
Rudder		
Area, A_R(m^2)	3.49	0.0155
Rudder aspect ratio, Λ	1.84	1.84
Rudder span, h(m)	2.57	0.171

$$T_E\dot{\delta} + \delta = -K_p(\psi - \psi_c) \qquad (13)$$

where the time constant T_E is 0.63 s. All other data needed for the numerical simulation including the hull geometry, hydrodynamic derivatives, rudder and propeller characteristics, roll viscous damping can be found in the Ref. [8].

In order to investigate the effect of GM on surf-riding and broaching, the numerical simulations of the fishing vessel with different GM values are conducted with various Froude numbers and wave directions. In the calculation cases, nominal Froude numbers are chosen from 0.30 to 0.45 while wave directions change from 0 to 15° with wave length to ship length λ/Lpp = 1.5 and wave steepness 0.055. Here 0° is defined as the following sea. The calculation cases are shown in Table 2.

Where "#" and "∗" denote the number for nominal Fn and wave direction. During the simulation, the ship is gradually accelerated from zero to the nominal Fn with the

Table 2. Calculation cases for numerical simulations

Case No.	GM(m)	Nominal Fn	Wave direction χ(deg)	λ/L_{pp}	Wave steepness H/λ
A-#-*	0.8	0.30–0.45	0–15	1.5	0.055
B-#-*	1.0	0.30–0.45	0–15	1.5	0.055
C-#-*	1.2	0.30–0.45	0–15	1.5	0.055

corresponding propeller rotation. The total simulation time for each case is set to be 120 s.

3.2 Comparison with Experiment Results

Firstly, the numerical model are validated through comparisons with existing experimental results of the ITTC ship A2 obtained from the literature [14]. In the literature, the surf-riding/broaching was intensively investigated through free-running model experiments under various GMs, wave lengths and wave steepness. In this research, the cases with GM = 1.0 m, λ/L_{pp} = 1.637 and H/λ = 0.1 are chosen for comparison as shown in Table 3.

Table 3. Calculation cases for numerical simulations

Case No.	GM(m)	Nominal Fn	Wave direction χ(deg)	λ/L_{pp}	Wave steepness H/λ
D-1-*	1.0	0.30	2,5,10,15,30	1.637	0.10
D-2-*	1.0	0.40	2,5,10,15,30	1.637	0.10
D-3-*	1.2	0.43	2,5,10,15,30	1.637	0.10

The comparisons between experiments and simulations on all the cases are presented in Fig. 3. From the figure, it can be found that periodic motions occur when Fn = 0.30 and 0.40 for both model experiments and numerical simulations. When Fn = 0.43, surf-riding and broaching occurs. For numerical simulations, broaching occurs for almost all the wave direction when Fn = 0.43, while surf-riding occurs under small wave direction for model experiments.

Moreover, the time histories for case No. D-3-3 with GM = 1.0 m, Fn = 0.40 and χ = 10° are compared between model experiment and numerical simulation as shown in Fig. 4. In the figure, broaching with large uncontrolled heading change and loss of stability can be observed from both experiment and simulation. Dispersions on the time when broaching occurs may be caused by the different initial conditions between experiment and simulation. Furthermore, simulated motion time histories of several other cases are demonstrated in Fig. 5, 6, and 7. Thus through the comparison with model experiments, it can be concluded that the proposed numerical model can predict surf-riding and broaching with certain accuracy.
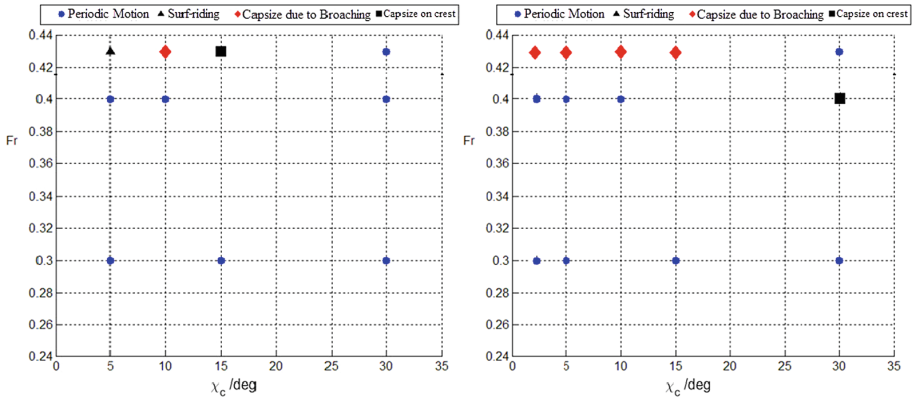
Fig. 3. Experiment and simulation results (Left: experiment, Right: simulation)
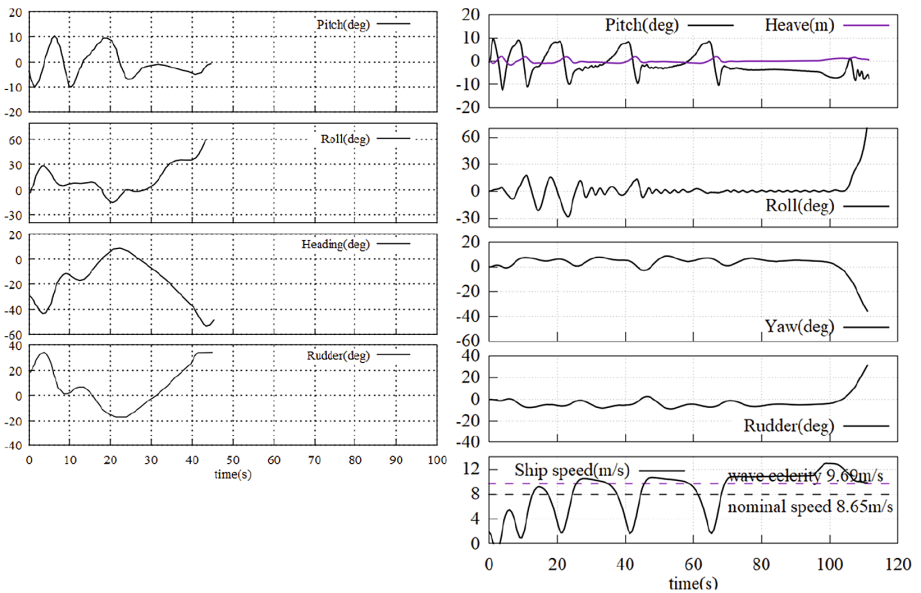

Fig. 4. Comparison on motion time histories of case No. D-3-3 with GM = 1.0 m, Fn = 0.40 and χ = 10° (Left: experiment, Right: simulation)

3.3   Simulation Results

The numerical simulations of the fishing vessel with GM = 1.0 m in following and quartering waves are conducted under the calculation cases described in the last section. Based on the simulation results, the ship motion responses are categorized and numbered into 5 types: (1) Periodic Motion, (2) Surf-riding, (3) Broaching after Surf-riding, (4) Capsize due to Broaching after Surf-riding and (5) Capsize on the wave crest. The motion responses of each type are demonstrated in Fig. 8, 9, 10, 11, and 12.
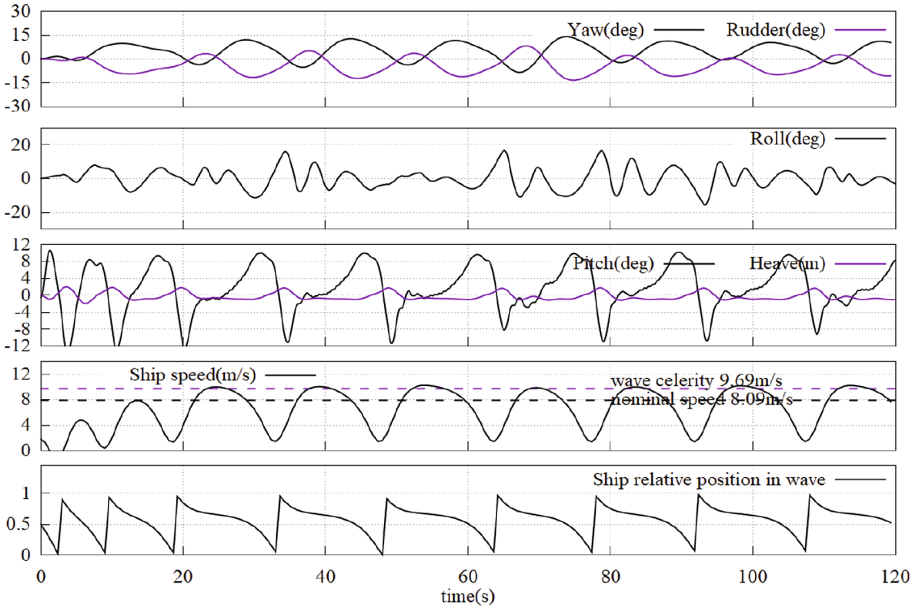
Fig. 5. Motion response of case D-2-3 with GM = 1.0 m, Fn = 0.40 and χ = 10°
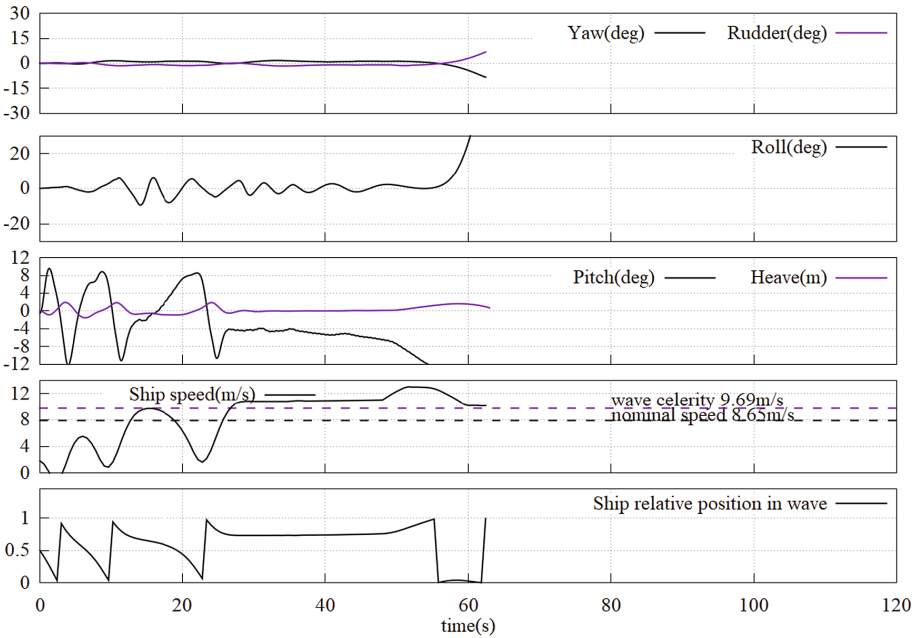
Fig. 6. Motion response of case D-3-1 with GM = 1.0 m, Fn = 0.40 and χ = 2°
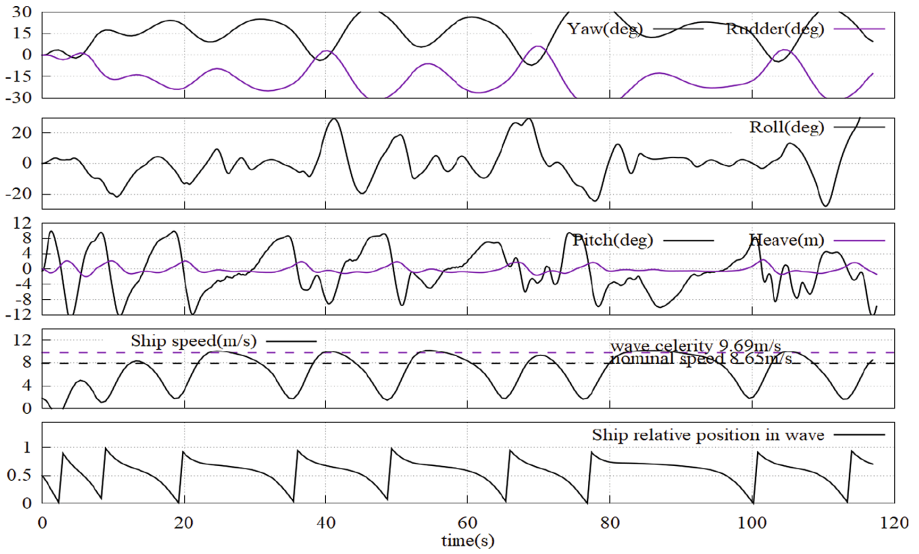
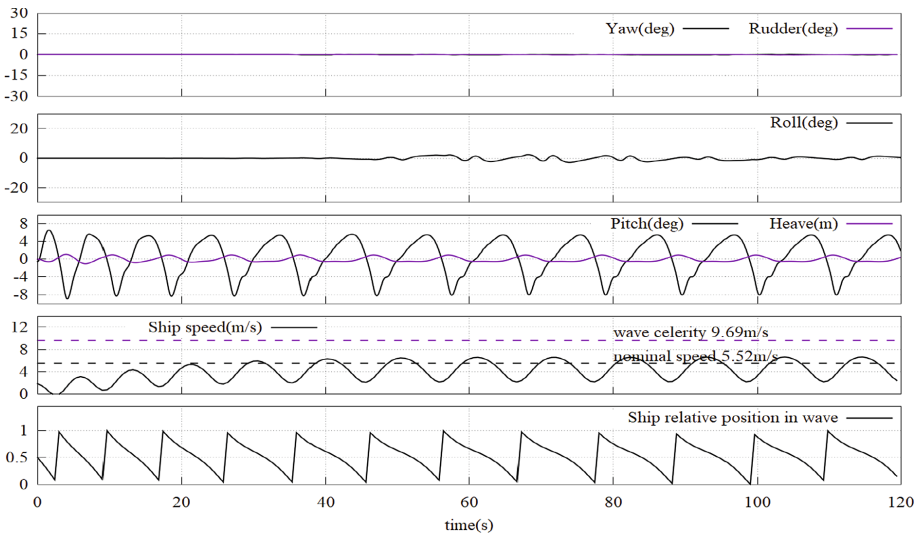**Fig. 7.** Motion response of case D-3-1 with GM = 1.0 m, Fn = 0.40 and χ = 30°

Fig. 8. Motion response of case B-1-0 with GM = 1.0 m, Fn = 0.30 and χ = 0°

Periodic Motion: In case B-1-0 with GM = 1.0 m, Fn = 0.30 and χ = 0°, the ship is doing periodic motion as shown in Fig. 3. Pitch, heave and surge are almost periodic.

Surf-Riding: In case B-10-0 with GM = 1.0 m, Fn = 0.39 and χ = 0°, surf-riding occurs as shown in Fig. 9. From the figure, it can be observed that the ship speed
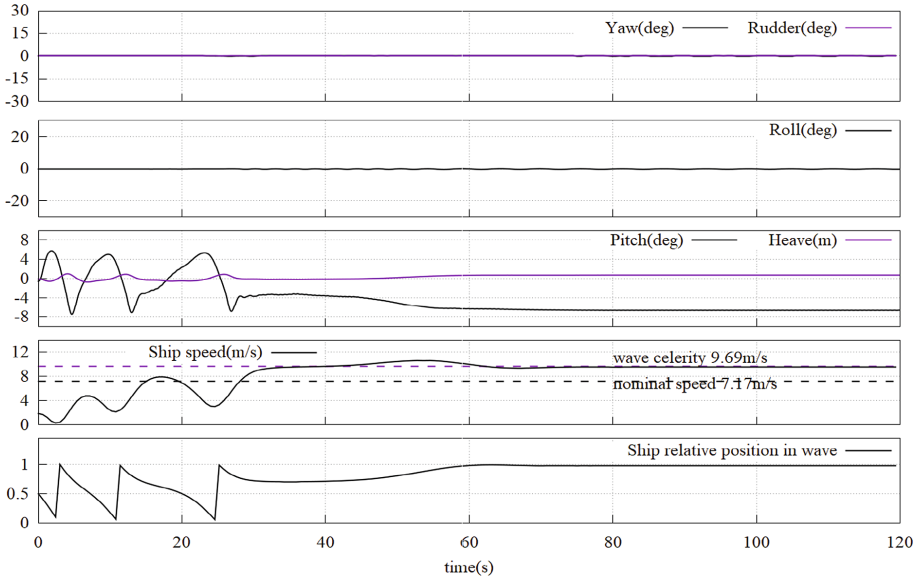
Fig. 9. Motion response of case B-10-0 with GM = 1.0 m, Fn = 0.39 and χ = 0°
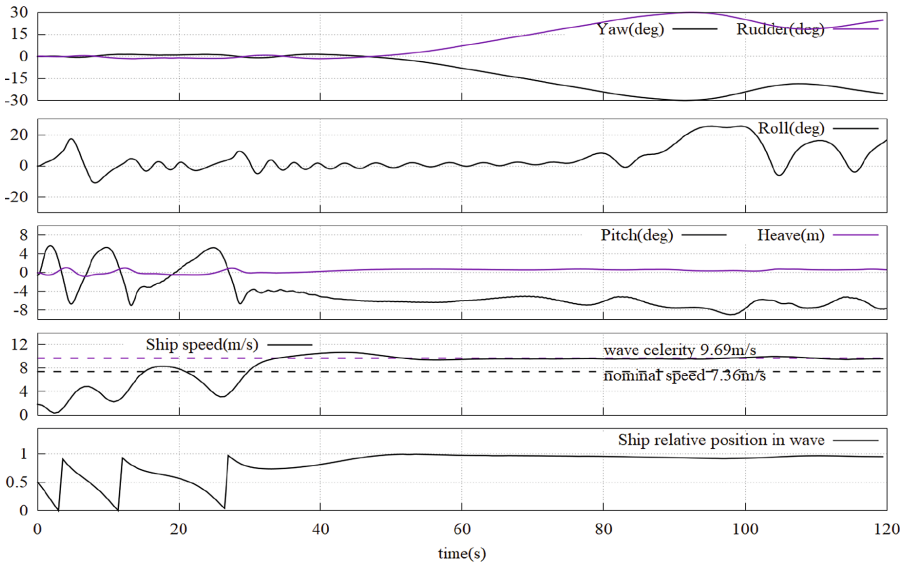
Fig. 10. Motion response of case B-11-02 with GM = 1.0 m, Fn = 0.40 and χ = 2°

reaches the wave celerity after around t = 30 s. The pitch angle and the ship relative position in wave keep almost constant, which indicate the occurrence of surf-riding.
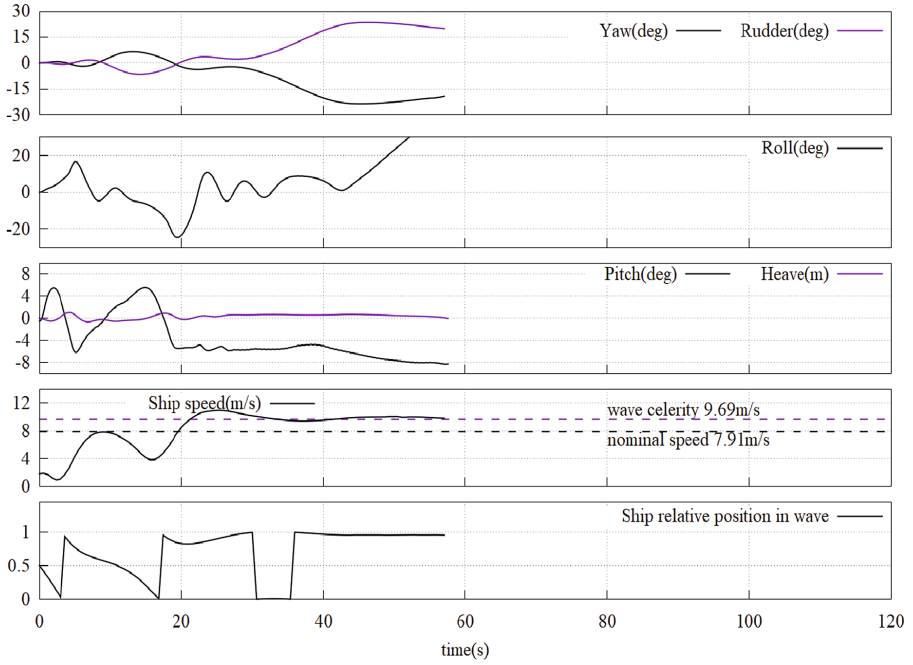
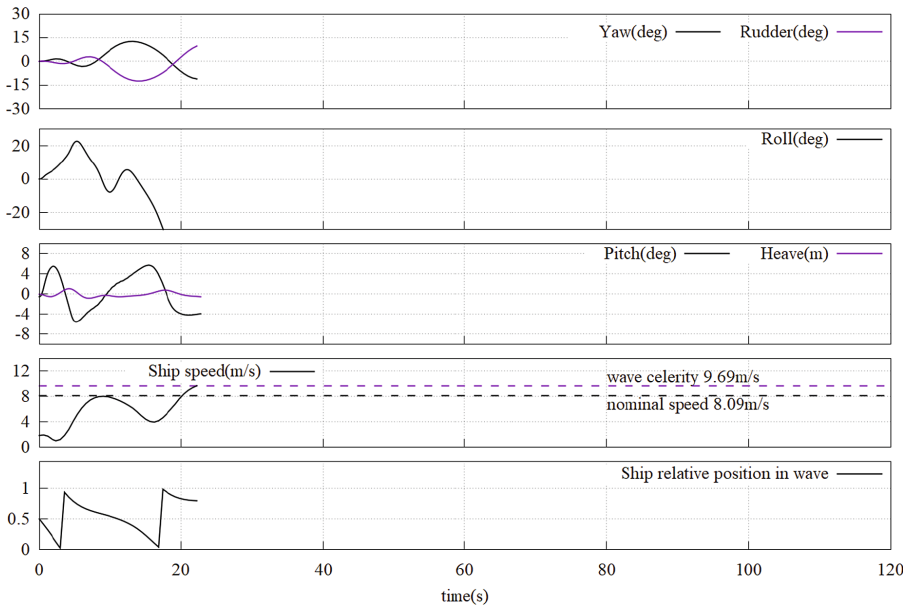**Fig. 11.** Motion response of case B-14-7 with GM = 1.0 m, Fn = 0.43 and $\chi = 7°$

Fig. 12. Motion response of case B-15-14 with GM = 1.0 m, Fn = 0.44 and $\chi = 14°$

Broaching After Surf-Riding: In case B-11-02 with GM = 1.0 m, Fn = 0.40 and $\chi = 2°$, the broaching occurs after surf-riding occurs as shown in Fig. 10. From the figure, it can be observed that the ship speed reaches the wave celerity around t = 30 s and surf-riding occurs. After surf-riding when t > 50 s, the heading angle increases very fast, despite rudder control is applied. After t > 80 s, the roll angle also grows suddenly. The broaching after surf-riding occurs. However, the ship doesn't capsize.

Capsize due to Broaching After Surf-Riding: In case B-14-7 with GM = 1.0 m, Fn = 0.43 and $\chi = 7°$, the broaching occurs after surf-riding occurs and leads to capsizing as shown in Fig. 11. From the figure, it can be observed surf-riding occurs after around t = 20 s. After surf-riding when t > 40 s, the heading angle increases very fast and broaching occurs. Then, the roll angle grows suddenly and the ship capsizes.

Capsize on the Wave Crest: In case B-15-14 with GM = 1.0 m, Fn = 0.44 and $\chi = 14°$, the ship capsizes on the wave crest due to reduction of restoring moment as shown in Fig. 12. No surf-riding and broaching occurs.

The simulation results are summarized and plotted in Fig. 13. In the figure, the 5 types of ship motions are plotted in different colors. It can be found from the figure that surf-riding and broaching occur as the nominal Fn increasing. The threshold Froude number Fn_{th} of surf-riding and broaching is around $Fn_{th} = 0.39$. The ship tends to capsize when the wave direction grows.
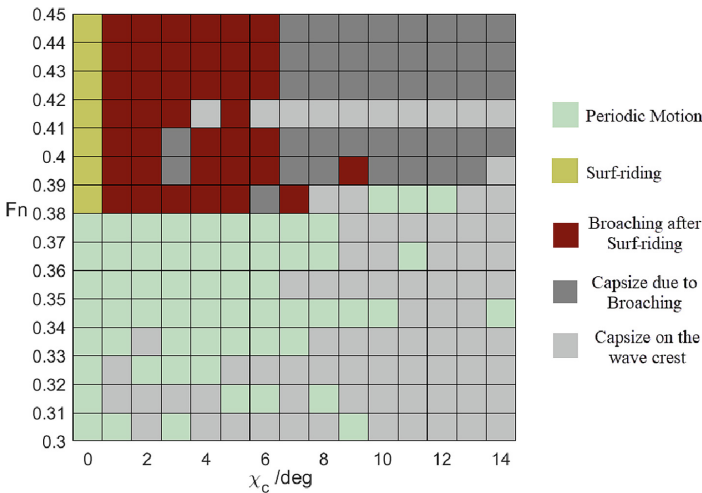

Fig. 13. Simulation results for GM = 1.0 m

4 Influence of GM

In order to investigate the influence of GM, the numerical simulations on the cases with GM = 0.8 and 1.2 m are conducted using the 6-DOF model. The simulation results are summarized and presented in Fig. 14 and 15.
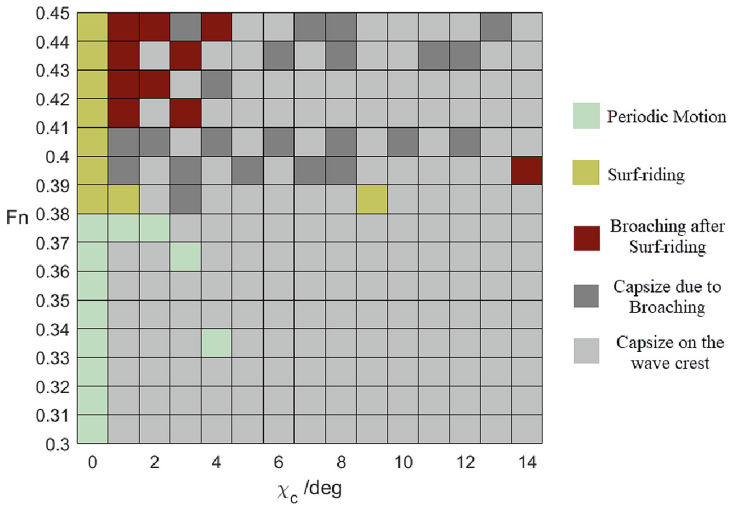

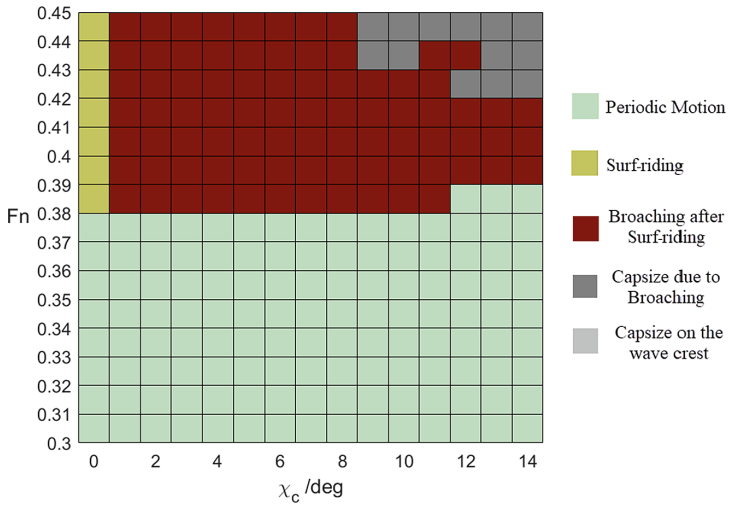**Fig. 14.** Simulation results for GM = 0.8 m

Fig. 15. Simulation results for GM = 1.2 m

Through the comparison on the simulation results of different GM values shown in Fig. 13, 14, and 15, It can be found that the change on GM value has significant influence on the occurrence of surf-riding and broaching. When GM = 0.8 m as in Fig. 14, capsize due to broaching and capsize on the wave crest are more easily to occur due to lack of enough roll restoring moment. The ship is vulnerable to capsizing. When GM increases as in Fig. 13 and 15, the area of capsizing decreases significantly. Almost no capsizing occurs even in large quartering waves when GM = 1.2 m. This conclusion is much similar to that of model experiment shown in Ref. [14] which also concluded that the area of broaching decrease significantly under large GM. Moreover, he threshold Froude numbers Fn_{th} of surf-riding in following seas for different GM values are the same which is around $Fn_{th} = 0.39$. Because the surf-riding in following seas is not affected be the transverse motion.

5   Conclusions

In this paper, the influence of the GM on surf-riding and broaching of the ITTC A2 fishing vessel are investigated using a 6-DOF numerical model. The numerical model is validated by comparisons with the model experiment described in Ref. [14]. Numerical simulations in following and quartering seas with various speeds, wave directions and GM values are conducted. Based on results of the numerical simulation, the following conclusions can be drawn.

The threshold Froude numbers Fn_{th} of surf-riding in following seas for different GM values are the same. However, the change on GM value has significant influence on the occurrence of broaching and capsizing. The ship is vulnerable to capsizing when GM = 0.8 m. Almost no capsizing occurs even in large quartering waves when GM = 1.2 m.

References

1. Davidson, K.S.M.: A note on the steering of ships in following seas. In: Proceedings of the 7th International Congress of Applied Mechanics, London, pp. 554–556 (1948)
2. Feng, P., Shen, X., Fan, S.: Study on the IMO second generation intact stability criteria of surf-riding/broaching failure mode. In: Proceedings of World Maritime Technology Conference 2015, Rhode Island, USA (2015)
3. Grim, O.: Das Schiff in von achtern auflaufender. Schiffbau-Versuchsanstalt (1951)
4. Gu, M., Chu, J., Han, Y., Lu, J.: Study on vulnerability criteria and model experiment for surf-riding/broaching. J. Ship Mech. **22**, 287–295 (2018)

5. Ikeda, Y., Himeno, Y.: Report of the Department of Naval Architecture University of Osaka Prefecture, A Prediction Method for ship Roll Damping (1978)

6. IMO SDC6/WP.6: Finalization of Second Generation Intact Stability Criteria, London, UK (2019)

7. Makov, Y.: Some results of theoretical analysis of surf-riding in following seas. Trans. Krylov Soc. **126**, 124–128 (1969)

8. NAOE Osaka University: Sample ship data sheet: ITTC A2 fishing vessel (2015). http://www.naoe.eng.osaka-u.ac.jp/imo/a2

9. Salvesen, N., Tuck, O.E., Faltinsen, O.: Ship motions and sea loads. SNAME Trans. **78**, 250–287 (1970). citeulike-article-id:10193407

10. Spyrou, K.J.: Dynamic instability in quartering seas: the behavior of a ship during broaching. J. Ship Res. **40**, 46–59 (1996)

11. Umeda, N.: Nonlinear dynamics of ship capsizing due to broaching in following and quartering seas. J. Mar. Sci. Technol. **4**, 16–26 (1999). https://doi.org/10.1007/s007730050003

12. Umeda, N., Hamamoto, M.: Capsize of ship models in following/quartering waves: physical experiments and nonlinear dynamics. Philos. Trans. R. Soc. Lond. Ser. A Math. Phys. Eng. Sci. **358**, 1883–1904 (2000). https://doi.org/10.1098/rsta.2000.0619

13. Umeda, N., Hashimoto, H.: Qualitative aspects of nonlinear ship motions in following and quartering seas with high forward velocity. J. Mar. Sci. Technol. **6**, 111–121 (2002). https://doi.org/10.1007/s007730200000

14. Umeda, N., Matsuda, A., Hamamoto, M., Suzuki, S.: Stability assessment for intact ships in the light of model experiments. J. Mar. Sci. Technol. **4**, 45–57 (1999). https://doi.org/10.1007/s007730050006

15. Yu, L., Ma, N., Fan, S., Feng, P., Gu, X.: Numerical simulation and experimental validation on the surfriding and broaching of a fishing vessel. In: Proceedings of the International Conference on Offshore Mechanics and Arctic Engineering – OMAE, Busan, Korea (2016)

16. Yu, L., Ma, N., Gu, X.: Numerical investigation into ship stability failure events in quartering seas based on time domain weakly nonlinear unified model. In: Proceedings of the 14th International Ship Stability Workshop, Kuala Lumpur, Malaysia, pp 229–235 (2014)

17. Yu, L., Ma, N., Gu, X.: Influence of rudder emersion on ship broaching prediction. In: 12th International conference on the Stability of Ships and Ocean Vehicles (2015)

18. Yu, L., Ma, N., Gu, X.: Design considerations for prevention of surf-riding and broaching of a fishing vessel. In: Proceedings of Practical Design of Ships and Other Floating Structures 2016, Copenhagen, Denmark (2016)

19. Yu, L., Ma, N., Gu, X.: On the mitigation of surf-riding by adjusting center of buoyancy in design stage. Int. J. Nav. Archit. Ocean Eng. **9**, 292–304 (2017). https://doi.org/10.1016/j.ijnaoe.2016.10.008